AIMS Energy, 12(1): 1–30.
DOI: 10.3934/energy.2024001
Received: 10 September 2023
Revised: 24 October 2023
Accepted: 30 October 2023
Published: 06 December 2023

http://www.aimspress.com/journal/energy

Research article

A chaotic Jaya algorithm for environmental economic dispatch incorporating wind and solar power

Vishal Chaudhary[1], Hari Mohan Dubey[2], Manjaree Pandit[1] and Surender Reddy Salkuti[3,*]

[1] Department of Electrical Engineering, MITS Gwalior 474005, India
[2] Department of Electrical Engineering, BIT Sindri, Dhanbad 828123, India
[3] Department of Railroad and Electrical Engineering, Woosong University, Daejeon 34606, Republic of Korea

* **Correspondence:** Email: surender@wsu.ac.kr; Tel: +821096741985; Fax: +82426296735.

Abstract: The integration of renewable energy resources (RESs) into the existing power grid is an effective approach to reducing harmful emission content. Environmental economic dispatch is one of the complex constrained optimization problems of power systems. These problems have become more complex as a result of integrating RESs, as the availability of solar and wind power is stochastic in nature. To obtain the solution of such types of complex constrained optimization problems, a robust optimization method is required. Literature shows that chaotic maps help to boost the search capability through improvisation in the exploration and exploitation phases of an algorithm; hence, they are able to provide superior solutions during optimization. Therefore, in this study, a new optimization technique was developed based on the Jaya algorithm called the chaotic Jaya algorithm. Here the main aim was to investigate the impact of RES integration into conventional thermal systems on total power generation cost and emissions released to the environment. The proposed approach was tested for two standard cases: (i) scheduling of a committed generating unit for a specific time and (ii) scheduling of a committed generating unit for a time period of 24 hours with 24 intervals of 1 hour each. The simulation results show that a tent map is the best-performing map for a sample problem under consideration, as it provides better results. Hence, it has been considered for detailed analysis.

Keywords: environmental economic dispatch; dynamic environmental economic dispatch; renewable energy resources; Jaya algorithm; chaotic map

1. Introduction

The need for electrical energy is growing day by day with industrial growth, and it will continue to increase due to widespread industrial growth. The electricity sector is still dominated by thermal power, in particular fossil fuels such as coal, natural gas and petroleum. They are considered the main sources of harmful pollution, and they have gained much attention in the last few decades. By considering new regulations for excessively generated greenhouse gases, a combination of economic dispatch and constraints on emission has come into existence; it is called economic emission dispatch (EED). EED is a multi-objective optimization problem of power systems, where in addition to the minimization of power generation cost, the minimization of emission is also considered simultaneously. The complicated operational constraints related to the EED problem, such as the valve-point loading effects, ramp-rate limits and prohibited operating zones (POZ) make the formulation highly nonlinear, discontinuous and non-convex. The main idea of EED is to find out the best compromise solution between two objectives i.e., cost and emission. The EED problem can be solved either by considering emission as a weighted function in the objective function [1–3] or by considering emission as a constraint [4]. Combined EED (CEED) is another method in which the coefficient of the price penalty factor is multiplied by the emission part of the objective function [5–7]. Also, a multi-objective optimization problem can be solved by converting it into a single-objective optimization problem using the weighted sum approach. The best part of the weighted sum method is that sets of Pareto-optimal solutions can be obtained by varying the weight [3].

As per the literature, deterministic approaches are not found to be suitable for dealing with large-scale integrated power systems. These methods are found to be associated with the inability to escape the local minima [8]. Therefore, researchers have turned toward nature-inspired optimization (NIO) methods due to their ability to find near-optimal solutions more efficiently. NIO methods knit together five categories of optimization approaches, i.e., evolutionary optimization, swarm intelligence-based optimization, ecology-based optimization, physical science-based optimization and optimization methods inspired by human intelligence [9].

Particle swarm optimization (PSO) is a well-accepted algorithm that belongs to the family of swarm intelligence algorithms due to its easy implementation, simplicity, fast convergence and robustness. However, PSO is very sensitive to its control parameters. A fuzzy section mechanism has been implemented and utilized for the solution to the multi objective economic dispatch (MOED) problem in [10]. To control the inertia weight an annealing reduction technique was implemented in [11]. The gravitational search algorithm (GSA) is based on Newton's law of gravity. It is a memory-less algorithm that can accelerate the optimization process without sacrificing accuracy. Obtaining the solution to multi-dimensional CEED problems by using a GSA is discussed in [5]. The harmony search algorithm (HSA) is a derivative-free optimization method inspired by the music improvisation of the musicians. In [6], the chaotic patterns and virtual memory concepts are utilized for solving the CEED problems; this modification is found to be highly efficient. The sine cosine algorithm is a population-based optimization method. It uses a mathematical model to create multiple initial random candidate solutions and requires them to fluctuate toward the best solution by utilizing sine and cosine functions. It has been applied and tested on CEED problems and found to be fast and efficient [7].

Literature shows that with the hybridization of two methods, proper balance between exploration and exploitation can be possible and will lead to improved performance.

Differential evolution (DE) is a heuristic method that improves candidate solutions over several generations by using three operations, i.e., mutation, crossover and selection, to reach an optimal solution. DE is found to give better solutions while satisfying all operational constraints for multimodal non-convex EED problems [12]. However, DE is unable to map its unknown variables efficiently when the complexity and size of the system increase. In the initial phase, the solution moves toward its optima in a faster manner; however, in a later stage, it requires fine-tuning. To achieve a proper balance between exploration and exploitation, a hybrid DE/biogeography-based optimization (BBO) method [13] has been used; it utilizes the migration operator of BBO, along with the three operators of DE, to find better convergence and solution quality. Similarly, by simultaneously updating the particle velocity in PSO and the acceleration coefficient of the GSA, improved performance was achieved [14]. By applying the time-variable acceleration coefficient in PSO to explore the entire search space and a local version of DE to the exploitation phase a hybrid DE-PSO algorithm [15] was used to obtain the feasible solution in a fast and efficient manner for a multi-objective economic dispatch (MOED) constraint optimization problem.

Rising power demand with minimum pollution constraints can be achieved through the integration of renewable energy sources (RESs) in the existing power network. However, the integration of RESs further complicates the problem due to their stochastic nature. RESs such as wind and solar power have maximum power generation limits that are variable and change with time. The uncertainty associated with RESs is a serious factor that must be considered for power generation planning for a longer time frame. The uncertainty function associated with RESs can be modeled by using the beta, log-normal, or Weibull probability distribution function (PDF). The solution to the EED problem for wind-thermal systems, as obtained by using a Weibull PDF is presented in [9,16–17]. Recently, in [18–20] solutions for EED were presented as a result of incorporating solar power. The binary flower pollination algorithm [18] has been applied to solve the CEED problem by incorporating solar power. Risk probability concepts were utilized to attain a better solar share of photovoltaic units and this reduced the total cost of the hybrid system. Impact analysis with a focus on the total operating cost and reduction in emission level of a solar-wind-thermal system was carried out by using a hybrid teaching-learning-based optimization (TLBO)-PSO algorithm in [19]. A new constrained multi-objective extremal optimization algorithm that has advanced constrained handling capability was proposed for the solution of the EED problem incorporating variable wind and solar power [20]. The lognormal PDF for calculating solar power, as well as the Weibull PDF for the calculation of wind power are utilized here.

Dynamic EED (DEED) is an extension of the EED problem, where the scheduling of committed generator units is carried out over the scheduled time period. Here, the ramping constraints of generators are also taken into consideration [3]. It is much more complex to solve than the classical EED problem due to the application of much more variable and operational constraints. In 2006, a PSO-based goal attainment method was used to solve the five-unit DEED problem. The multi-objective problem has been converted to single objective optimization goal attainment and then solved by using PSO [21]. PSO with avoidance of worst locations (AWL) and gradually increasing directed neighborhoods (GIDN) has been used to solve the 10-unit DEED problem. In the aforementioned study, a weighted sum approach was applied to convert the multi-objective problem into a single objective problem. The simulation results demonstrated that the performance of PSO with GIDN topology and AWL performs best [22]. The non-dominated sorting genetic algorithm II (NSGA II) was applied to solve 10 DEED problems with non-smooth cost and emission functions [23]. In their

study, the NSGA simulation results were found to be better than those for the classical approach. To improve the computational efficiency of the bacterial foraging algorithm (BFA), a BFA with a crossover operation and parameter automation strategy has been used to solve the 10-unit DEED problem [24]. Finally, the fuzzy selection mechanism was adopted to find non-dominating solutions. In this previous study, the simulation results show that an improved BFA performs better than the classical BSA and NSGA-II. To avoid entrapment in local optima, TLBO phase angle-based mechanisms have been proposed and applied to solve 5-, 10- and a large-scale 120-unit DEED problem [25]. Simulation results demonstrate that Θ-TLBO was able to provide high-quality well-distributed solutions in a single run. Variants of DE like multi-objective neural networks evolved with DE [26] to generate the Pareto front and the efficient fitness-based DE [27] which has a double mutation strategy, random mutation factor and crossover rate with learning ability have been proposed to solve DEED problem. In [28], a new enhanced harmony search algorithm was used to solve the DEED problem that utilizes (i) three arbitrary distance bandwidths to enhance global and local search capability and (ii) consideration of both the best and worst memory vectors in the second half of generation to enhance solution quality and avoid premature convergence.

Considering the ever-increasing power demand, fossil fuel costs and environmental legislation (e.g., Kyoto protocol) have forced expansion of the use of RESs. Hence, hybrid power generating systems come into existence. For this, a collective cost function of conventional thermal power generators with RESs and emission function needs to be investigated to analyze its impact on environmental and economic factors. The power generation by RES like wind and solar both is uncertain and variable. Therefore, direct cost, overestimation and underestimation costs are considered in the modeling. However, the uncertainty of RES leads to more complications in the formulation of the DEED problem [29–31]. A hybrid flower pollination algorithm that combines flower pollination algorithm (FPA) and DE is used to solve the DEED problem of a six-unit wind-thermal system [29]. Here fuzzy selection was used to find better trade-off solutions. Whale optimization algorithm (WOA) which is inspired by the hunting strategy of humpback whales [30], DE with ensemble selection method [31] was used to handle the DEED problem with wind integration. Substantial saving in cost and emission is reported in [32] using electric vehicles and a multi-objective evolutionary approach known as the exchange market algorithm. The membrane optimization algorithm is employed for the solution of the combined cost-emission optimization problem and produces Pareto solutions and recommendations for the best solution which is superior to reported results [33]. In reference [34] Equilibrium optimization was used for profit maximization as well as reduction in pollution content. It was tested on a hybrid thermal-wind-PV system.

PV systems and wind turbines both are dependent on climate change and hence neither system is capable of delivering enough electricity reliably and efficiently. However, a Battery storage system with its integration in a suitable size helps to improve power quality, suppresses power due to renewable energy resources and also helps to reduce the mean cost of energy [35,36].

According to the no-free-lunch (NFL) theorem, no algorithm can solve all types of optimization problems and there is still a chance to get a better solution by a new algorithm [37]. Also, literature shows that chaotic sequences with heuristic optimization have been used together to get improved performance [38,39].

Mostly the reported methods used to solve CEED/DEED problems have some limitations as trapping to local optima, slow convergence and complexity due to more control parameters. JAYA algorithm is selected due to the fewer control parameters to tune and easier implementation. Chaotic

map with JAYA is used to avoid trapping to local optima. The main contribution in this work is summarized as follows:

- An analytical objective function model is developed for a hybrid thermal-wind-solar system. It includes the collective cost function of three types of power generating units, operational constraints, uncertainty of wind, solar system and emission function due to thermal units.
- Population-based JAYA algorithm and JAYA algorithm embedded with a chaotic map are implemented to investigate the hybrid thermal-wind-solar for CEED and DEED problems.
- The impact of wind integration, with both solar and wind integration is investigated with a 10-thermal unit non-convex system and analyzed for single and bi-objective optimization under fixed load demand.
- The competence and robustness of the proposed methodology are confirmed with the reported results.
- The impact of wind integration, both solar and wind integration is investigated with 10-thermal units analyzed for single and bi-objective optimization for 24 hours with 24 intervals of 1 hour each.

Problem formulation is presented in Section 2. A brief introduction of the JAYA algorithm, chaos maps and step-by-step implementation process of the Ch-JAYA algorithm for the solution of the EED problem are discussed in section 3. The simulation results and discussions are presented in section 4 and finally, concluding remarks are drawn in section 5.

2. The mathematical formulation of the DEED problem

The objective of the DEED problem is to find out the optimal generation schedule over the period in such a manner that costs associated with power generation and emission are minimized simultaneously. The total cost (*TC*) of power generation can be symbolically represented by,

$$TC = \sum_{h=1}^{H} \left\{ \sum_{k=1}^{N_{th}} C(P_{thk})_h + \sum_{l=1}^{N_w} C(P_{wl})_h + \sum_{m=1}^{N_{pv}} C(P_{pvm})_h \right\} \quad (1)$$

The first part of Eq (1) represents the fuel cost of the thermal power generating unit, and it is given by,

$$\sum_{k=1}^{N_{th}} C(P_{thk}) = \sum_{k=1}^{N_{th}} [a_k P_{thk}^2 + b_k P_{thk} + c_k + \left| e_k \sin\left(f_k\left(P_{thk}^{min} - P_{thk}\right)\right)\right|] \quad (2)$$

The second part of Eq (1) is the cost due to wind power. The system operator has to deal with either for deficit or more than scheduled power generation by wind farms due to the stochastic nature of wind power. The deficit in wind power can be fulfilled by maintaining a sufficient amount of spinning reserve (SR) and it is considered as an overestimation and the cost corresponding to SR is added to power generation. On the other hand, the generation of more power than scheduled power by wind farm system operators has to bear the penalty called underestimation cost. Therefore, wind power generation includes three costs: direct cost, overestimation cost/reserve cost and underestimation cost/penalty cost [3,20,29–31].

$$\sum_{l=1}^{N_w} C(P_{w,l}) = \sum_{l=1}^{N_w} (b_{w,l} \times P_{ws,l}) + \sum_{l=1}^{N_w} k_p\left(P_{wav,l} - P_{ws,l}\right) + \sum_{l=1}^{N_w} k_r (P_{ws,l} - P_{wav,l}) \quad (3)$$

Reserve cost/overestimation cost of wind power is given by,

$$k_r\left(P_{ws,l} - P_{wav,l}\right) = k_r \times \int_0^{P_{ws,l}} (P_{ws,l} - P_{w,l}\,)\, f_w(P_w) dP_w \tag{4}$$

The penalty cost/underestimation cost of wind power is given by,

$$k_p\left(P_{wav,l} - P_{ws,l}\right) = k_P \times \int_{P_{ws,l}}^{P_{wrl}} (P_{w,l} - P_{ws,l})\, f_w(P_w) dP_w \tag{5}$$

In this work, the Weibull PDF is used for wind speed distribution as the wind speed is uncertain and irregular. The Weibull PDF is represented by,

$$f(v) = \left(\frac{k}{c}\right) \times \left(\frac{v}{c}\right)^{k-1} \times \exp\left[-\left(\frac{v}{c}\right)^{k}\right] \tag{6}$$

The corresponding cumulative distribution function (CDF) can be represented by,

$$F(v) = 1 - \exp\left[-\left(\frac{v}{c}\right)^{k}\right] \tag{7}$$

For each wind power generating unit, the power output at a given wing speed can be expressed by using [29–30,37],

$$P_w(v) = \begin{cases} 0 & v < v_{in} \quad and \quad v > v_{out} \\ \mathrm{P_{wr}}\left(\frac{v - v_{in}}{v_r - v_{in}}\right) & ; \quad v_{in} < v < v_r \\ \mathrm{P_{wr}} & ; \quad v_r < v < v_{out} \end{cases} \tag{8}$$

The probability of wind power is 0 to $\mathrm{P_{wr}}$, and it can be calculated by using,

$$f_w(\mathrm{P_w})\{\mathrm{P_w} = 0\} = 1 - exp\left(-\left(\frac{v_{in}}{c}\right)^{k}\right) + exp\left(-\left(\frac{v_{out}}{c}\right)^{k}\right) \tag{9}$$

Wind power in the range $v_{in} < v < v_r$ is given by [37],

$$\mathcal{P} = \mathrm{P_{wr}}\left(\frac{v - v_{in}}{v_r - v_{in}}\right) = \left(\frac{\mathrm{P_{wr}}}{v_r - v_{in}}\right) \times v - \left(\frac{v_{in}}{v_r - v_{in}}\right) \tag{10}$$

$$f_w(\mathrm{P_w}) = \frac{k \times \hbar \times v_{in}}{P_{wr} \times c} \left(\frac{\left(1 + \frac{\hbar \times \mathcal{P}}{\mathrm{P_{wr}}}\right) v_{in}}{c}\right)^{k-1} \times exp\left\{-\left(\frac{\left(1 + \frac{\hbar \times \mathcal{P}}{\mathrm{P_{wr}}}\right) v_{in}}{c}\right)^{k}\right\} \tag{11}$$

where

$$\hbar = \left(\frac{v_r}{v_{in}}\right) - 1 \tag{12}$$

$$f_w(\mathrm{P_w})\{P_w = P_{wr}\} = exp\left(-\left(\frac{v_r}{c}\right)^{k}\right) - exp\left(-\left(\frac{v_{out}}{c}\right)^{k}\right) \tag{13}$$

A typical Weibull PDF with a shape factor of 2 and scale factors of 5 and 10 is shown in Figure 1. The third part of Eq (1) represents the cost associated with solar power. It also has three cost components including direct cost, reserve cost and penalty cost [40].

$$\sum_{m=1}^{N_{pv}} C(P_{pv,m}) = \sum_{m=1}^{N_{pv}} (b_{pv,m} \times P_{pvs,m}) + \sum_{m=1}^{N_{pv}} k_p\left(P_{pvav,m} - P_{pvs,m}\right) + \sum_{m=1}^{N_{pv}} k_r(P_{pvs,m} - P_{pvav,m}) \quad (14)$$

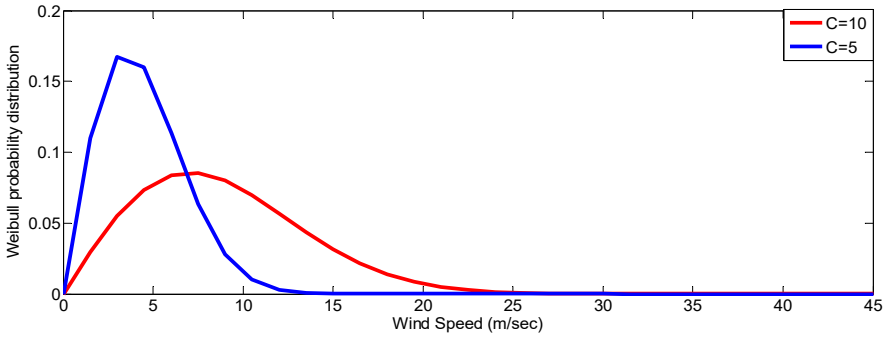

Figure 1. Weibull probability density function (PDF) for k = 2 and C = 5, 10.

Reserve cost associated with solar power generation that is derived from the overestimation of solar power and it can be represented by using [40],

$$k_r\left(P_{pvs,m} - P_{pvav,m}\right) = k_r \times \int_0^{P_{pvs,m}} (P_{pvs,m} - P_{pv,m}) f_{pv}\left(P_{pv}\right) dP_{pv} \quad (15)$$

Penalty cost associated with solar power generation is derived from the underestimation of solar power and it can be represented by using [40],

$$k_p\left(P_{pvav,m} - P_{pvs,m}\right) = k_p \times \int_{P_{pvs,m}}^{P_{pvr,m}} (P_{pv,m} - P_{pvs,m}) f_{pv}\left(P_{pv}\right) dP_{pv} \quad (16)$$

The solar irradiation (G_{pv}) to energy conversion function of solar PV generators can be represented as [40],

$$P_{pv}\left(G_{pv}\right) = \begin{cases} \mathrm{P_{pvr}} \times \left(\frac{{G_{pv}}^2}{G_{std} \times R_c}\right), & \text{for} \quad 0 < G_{pv} < R_c \\ \mathrm{P_{pvr}} \times \left(\frac{G_{pv}}{G_{std}}\right), & \text{for} \quad G_{pv} > R_c \end{cases} \quad (17)$$

The output of a solar power plant depends on irradiation at a particular location which can be modeled by Beta, Weibull, or Lognormal distribution. Here, Weibull PDF is used and it is represented by using [40],

$$f\left(G_{pv}\right) = \omega \times \left(\frac{k_1}{c_1}\right) \times \left(\frac{G_{pv}}{c_1}\right)^{k_1 - 1} \times \exp\left[-\left(\frac{G_{pv}}{c_1}\right)^{k_1}\right] + (1 - \omega) \times \left(\frac{k_2}{c_2}\right) \times \left(\frac{G_{pv}}{c_2}\right)^{k_2 - 1} \times \exp\left[-\left(\frac{G_{pv}}{c_2}\right)^{k_2}\right] \quad (18)$$

The cumulative distribution function (CDF) of Eq (18) can be represented by using,

$$F\left(G_{pv}\right) = \omega \times \left[1 - exp\left\{-\left(\frac{G_{pv}}{c_1}\right)^{k_1}\right\}\right] + (1 - \omega) \times \left[1 - exp\{-\left(\frac{G_{pv}}{c_2}\right)^{k_2}\}\right] \quad (19)$$

As per the transformation of the random variable, linear transformation is carried out with solar irradiation (G_{pv}) random variable, and it can be represented by using [40],

$$P_{pv} = aG_{pv} + \mathscr{b} = \Gamma(G_{pv}) \tag{20}$$

$$f_{pv}(P_{pv}) = f\left[\Gamma^{-1}(P_{pv})\right]\left|\frac{d\Gamma^{-1}(P_{pv})}{dP_{pv}}\right| = f(G_{pv}) \times \left|\frac{1}{a}\right| = f(G_{pv}) \times \left|\frac{P_{pv}-\mathscr{b}}{a}\right| \times \left|\frac{1}{a}\right| \tag{21}$$

Solar power probability for the piecewise function can be represented by using,

$$P_{pv} = G_{pv} \times \left(\frac{P_{pvr}}{G_{std}}\right) = aG_{pv} \text{ for } G_{pv} > R_c \tag{22}$$

where

$$a = \frac{\mathrm{P_{pvr}}}{G_{std}} \tag{23}$$

$$f_{pv}(P_{pv}) = f_{pv}\left(\frac{P_{pv}}{a}\right) \times \frac{1}{a} = f_{pv}\left(\frac{P_{pv}.G_{std}}{P_{pvr}}\right) \times \frac{G_{std}}{P_{pvr}} \tag{24}$$

The second-order transformation is accomplished with solar irradiation (G_s), and it can be represented by using,

$$P_{pv} = {G_{pv}}^2 \times \left(\frac{P_{pvr}}{G_r \times R_c}\right) = a^2 G_{pv} \text{ ; for } \quad 0 < G_{pv} < R_c \tag{25}$$

$$f_{pv}(P_{pv}) = \frac{1}{2\sqrt{aP_{pv}}}\left[f\left(\sqrt{\frac{P_{pv}}{a}}\right) + f\left(-\sqrt{\frac{P_{pv}}{a}}\right)\right] \tag{26}$$

$$f(P_{pv}) = \frac{1}{2\sqrt{\frac{\mathrm{P}_{pvr}P_{pv}}{G_{std}R_c}}} \times \left[f\left(\sqrt{\frac{P_{pv}G_{std}R_c}{\mathrm{P}_{pvr}}}\right) + f\left(-\sqrt{\frac{P_{pv}G_{std}R_c}{\mathrm{P}_{pvr}}}\right)\right] \tag{27}$$

The total emission (TE) from various pollutants can be symbolically represented as follows:

minimize

$$TE = \sum_{i=1}^{N_{th}} E_i(P_i) \tag{28}$$

where

$$E_i(P_i) = \alpha_i P_i^2 + \beta_i P_i + \gamma_i + \eta_i \exp\left(\delta_i . P_i\right) \tag{29}$$

The multi-objective optimization problem was converted into a single-objective optimization problem using the weighted sum approach [3]. The objective of the DEED problem can be written as,

minimize

$$[w \times TC + (1-w) \times TE]; \text{ where } w \in (0,1) \tag{30}$$

Subjected to the following operational constraints.

2.1. Operational constraints

These constraints are expressed as,

$$\sum_{k=1}^{N_{th}} P_{th,k} + \sum_{l=1}^{N_w} P_{w,l} + \sum_{m=1}^{N_{pv}} P_{pv,m} = P_D + P_L \tag{31}$$

$$P_{th,k}^{min} \leq P_{th} \leq P_{th,k}^{max} \tag{32}$$

$$P_{w,l}^{min} \leq P_{w,l} \leq P_{w,l}^{max} \tag{33}$$

$$P_{pv,m}^{min} \leq P_{pv,m} \leq P_{pv,m}^{max} \tag{34}$$

$$-RRL_{th,k}^{down} \leq P_{th,k} - P_{(th-1)k} \leq RRL_{th,k}^{up} \tag{35}$$

2.2. Ranking approach

To aggregate two conflicting objectives (cost and emission), the fuzzy-min ranking method is used. Linear membership function $\mu_{i,r}$ (i^{th} solution of r^{th} objective function) is described for each objective function F_i in Eq (36) and also in Figure 2.

$$\mu_{i,r} = \begin{cases} 1 & if \quad F_{i,r} \leq F_r^{min} \\ \frac{F_r^{max} - F_{i,r}}{F_r^{max} - F_r^{min}} & if \quad F_r^{min} \leq F_{i,r} \leq F_r^{max} \\ 0 & if \quad F_{i,r} \geq F_r^{max} \end{cases} \tag{36}$$

For i^{th} solution, the rank is defined as [24],

$$fuzzy\_min_i = \min(\mu_{i,r}) \qquad for \quad r = 1,2 \ldots . m \tag{37}$$

The solution with maximum membership value (μ_r) is considered as the best compromise solution (BCS).

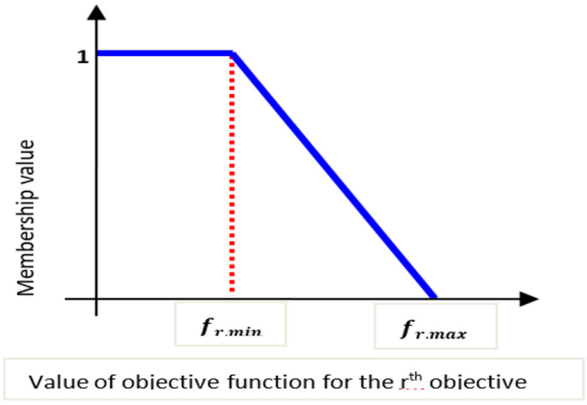

Figure 2. Membership function.

3. Chaotic JAYA algorithm

3.1. Jaya algorithm

The Jaya algorithm is one of the simple and powerful optimization methods proposed by Rao [41]. The basic idea behind the Jaya algorithm is to obtain a solution for a specified optimization problem that avoids the worst solution and moves toward the best one. It is a population-based evolutionary algorithm and does not require any algorithm-specific parameter to tune for its convergence.

Let us consider an objective function $f(X)$, where X is a d-dimensional variable and the population size is p. Let the best and worst values of the objective function produced by the candidate solution be $f(X_{best})$ and $f(X_{worst})$, respectively [39]. Then, the j^{th} element of the i^{th} solution is updated by using,

$$X^{n+1}{}_{ij} = X^{n}{}_{ij} + r_{1,ij} \times \left(X_{best,ij} - |X_{ij}|\right) - r_{2,i,j} \times \left(X_{worst,ij} - |X_{ij}|\right) \tag{38}$$

where $r_{1,ij}$ and $r_{2,i,j}$ are the two random numbers in the range [0,1].

The second term of Eq (38) helps to move solutions towards the best solution and the third term helps to escape away from the worst solution. All the improved objective function values at the end of every iteration are transferred to successive iterations. Hence, the algorithm can achieve victory by attending to the global best solution. This process carries forward the victorious members of the population through the iterations. Therefore, the algorithm has been named as Jaya which means victory in the Sanskrit and Hindi languages.

3.2. Chaotic JAYA algorithm

The search process of the Jaya algorithm is governed by the two uniformly distributed random numbers $r_{1,ij}$ and $r_{2,i,j}$. The Jaya algorithm was found to saturate prematurely for practical real-life problems where the objective functions have non-convex and discontinuous nature and there are probabilistic variables. From the literature, it was found that the random numbers generated using chaotic sequences enhance the population diversity and the global search capability of evolutionary

algorithms [6,24,36–37] thus avoiding convergence to the local optimum solution. Different chaotic maps were used to generate a sequence of chaotic random numbers introduced to replace two random numbers. The j^{th} element of the i^{th} modified solution vector in the $(n+1)^{th}$ iteration will be computed by using

$$X_{ij}^{n+1} = X_{ij}^{n} + Ch^{n+1} \times \{r_{1,ij} \times (X_{best,ij} - |X_{ij}|) - r_{2,i,j} \times (X_{worst,ij} - |X_{ij}|)\} \quad (39)$$

where Ch^{n+1} is the random number generated by using a chaotic map as explained in the next section. The solution strategy used for the optimization process using the Chaotic Jaya algorithm is presented using the flowchart in Figure 3.

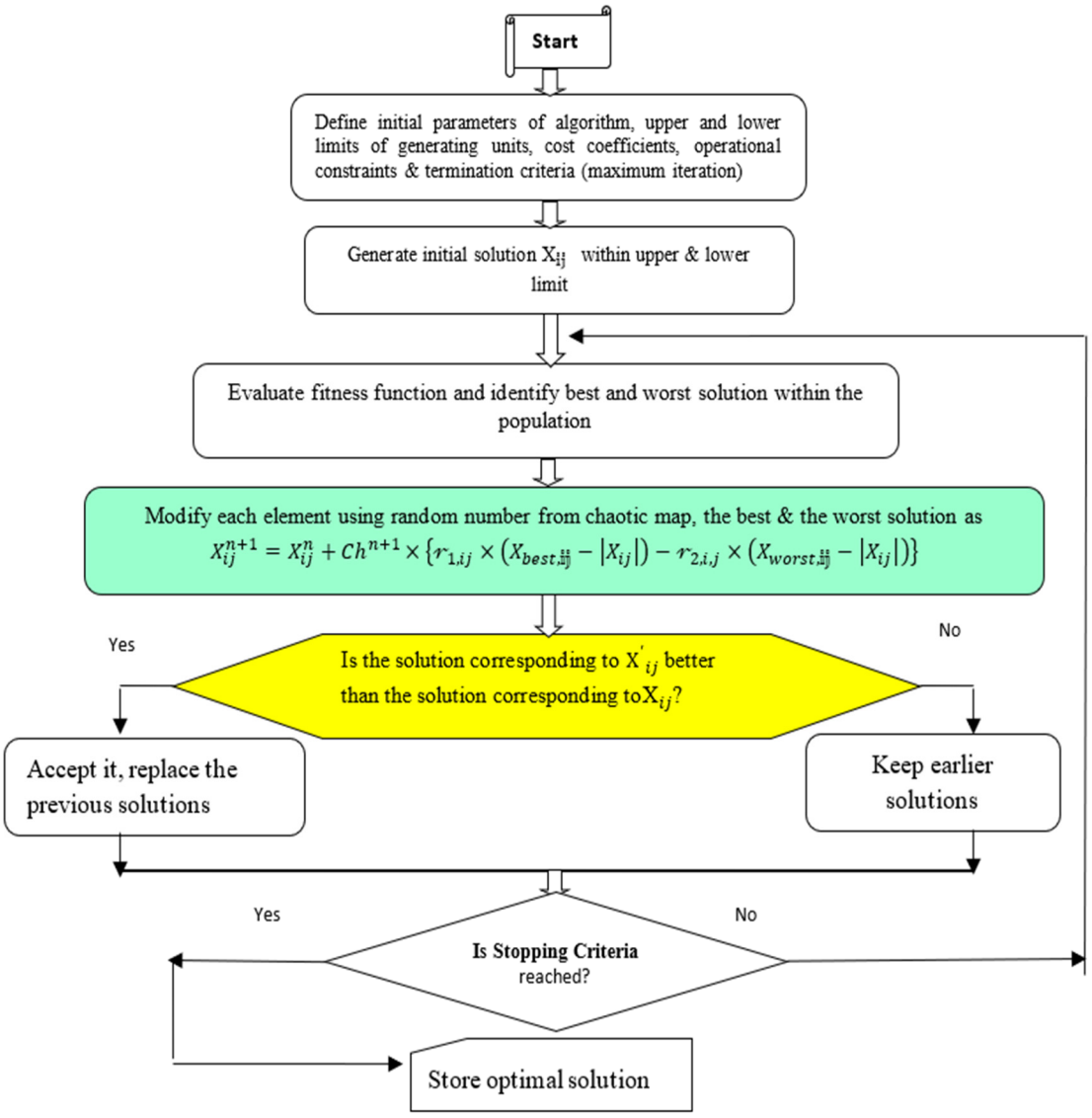

Figure 3. Flow chart for Ch-Jaya algorithm.

3.3. Chaotic map embedded with JAYA algorithm

Chaos theory is a branch of mathematics that deals with nonlinear dynamic systems and chaos systems are found to be highly sensitive to the initial condition. Chaos helps to improve the performance of population-based metaheuristic algorithms. The ten chaos maps [36,37] which are embedded with the Jaya algorithm are listed below. For n = 1, $\mathcal{X}_n = rand$.

3.1.1. Chebyshev map

$$\mathcal{X}_{n+1} = Cos(nCos^{-1}(\mathcal{X}_n)) \tag{40}$$

3.1.2. Circle map

$$\mathcal{X}_{n+1} = mod\{\mathcal{X}_n + \mathcal{b} - \left(\frac{a}{2\pi}\right) \times \sin(2\pi\mathcal{X}_n), 1), \qquad a = 0.5, \quad \mathcal{b} = 0.2 \tag{41}$$

3.1.3. Gauss/mouse map

$$\mathcal{X}_{n+1} = \begin{cases} 1, & \mathcal{X}_n = 0 \\ \frac{1}{mod(\mathcal{X}_n, 1)}, & otherwise \end{cases} \tag{42}$$

3.1.4. Iterative map

$$\mathcal{X}_{n+1} = Sin\left(\frac{a\pi}{\mathcal{X}_n}\right), \quad a \in (0,1) \tag{43}$$

here, the range of the map is (–1, 1).

3.1.5. Logistic map

$$\mathcal{X}_{n+1} = a\mathcal{X}_n(1 - \mathcal{X}_n), \quad a = 4 \tag{44}$$

3.1.6. Piecewise map

$$\mathcal{X}_{n+1} = \begin{cases} \frac{\mathcal{X}_n}{\mathcal{P}} & 0 \le \mathcal{X}_n < P \\ \frac{\mathcal{X}_n - \mathcal{P}}{0.5 - \mathcal{P}} & \mathcal{P} \le \mathcal{X}_n < \frac{1}{2} \\ \frac{1 - \mathcal{P} - \mathcal{X}_n}{0.5 - \mathcal{P}} & \frac{1}{2} \le \mathcal{X}_n < (1 - \mathcal{P}) \\ \frac{1 - \mathcal{X}_n}{\mathcal{P}} & (1 - \mathcal{P}) \le \mathcal{X}_n < 1 \end{cases} \tag{45}$$

here $\mathcal{P}$ is the control parameter considered as 0.4.

3.1.7. Sine map

$$\mathcal{X}_{n+1} = (\frac{a}{4}) \times Sin(\pi \mathcal{X}_n), \quad where \quad 0 < a \leq 4 \tag{46}$$

3.1.8. Singer map

$$\mathcal{X}_{n+1} = \mu(7.86\mathcal{X}_n - 23.31\mathcal{X}_n^2 + 28.75\mathcal{X}_n^3 - 13.1302875\mathcal{X}_n^4), \quad \mu = 1.7 \tag{47}$$

3.1.9. Sinusoidal map

$$\mathcal{X}_{n+1} = a\mathcal{X}_n^2 \times Sin(\pi \mathcal{X}_n), \quad where \quad a = 2.3 \tag{48}$$

3.1.10. Tent map

$$\mathcal{X}_{n+1} = \begin{cases} \frac{\mathcal{X}_n}{0.7} & \mathcal{X}_n < 0.7 \\ \left(\frac{10}{3}\right) \times (1 - \mathcal{X}_n) & \mathcal{X}_n \geq 0.7 \end{cases} \tag{49}$$

3.4. Implementation of chaotic JAYA algorithm for environmental economic dispatch

To verify the effectiveness of the Ch-JAYA algorithm for the solution of the EED problem, first define the experimental data like the number of power generating units as the dimension of the problem, cost coefficients, emission cost coefficients, min-max limit of power generating units, operational constriction, population size and maximum iteration as stopping criteria.

Step 1: Initialize the population randomly within upper and lower power generation limits as below:

$$P_i = \mathrm{P}_i^{min} + r \times \left(\mathrm{P}_i^{max} - \mathrm{P}_i^{min}\right) \qquad where \ i = 1,2,\dots,N \tag{50}$$

where $r \in [0,1]$ is a random number and N is the number of power-generating units.

Step 2: Calculate the total cost for each candidate solution using Eq (1), check for all associated operational constraints by using the Eqs (31−35), identify the best and worst solutions and preserve them.

Step 3: This process indicates the modification process of the algorithm. Modification of each power generating unit has been carried out as per Eq (39).

$$P^{\mathrm{new}}{}_i = \mathrm{P}_i + \mathrm{Ch} \times [rand_1 \times \left(\mathrm{P}_{best,i} - |P_i|\right) - rand_2 \times \left(P_{worst,i} - |P_i|\right)] \tag{51}$$

This step helps to move a solution towards the best solution and away from the worst one. The chaotic term Ch, acts as a scaling factor to ensure good diversification during the optimization process. The new best solution P_{best}^{new} and the new worst solution P_{worst}^{new} are preserved for use in the next iteration.

Step 4: Calculate the total cost for a modified solution after each iteration. All operational constraints given by Eqs (31−35) are checked for violations if any. The violations are used to convert

the constrained optimization problem into an unconstraint problem by using the penalty function approach. Thus, a feasible solution gets a better fitness as compared to an infeasible solution.

Step 5: If the updated solution is found to be better, then replace the modified solutions with previous solutions otherwise retain the previous one. The best solutions are stored when the stopping criterion is reached.

Step 6: Similarly, compute all Pareto optimal solutions and rank them based on $fuzzy\_min$ to get the best possible solution by using Eqs (36) and (37).

4. Case studies, results and discussion

The proposed approach for the solution of the EED problem with the integration of RESs has been implemented using an improved version of the Jaya algorithm. The proposed Ch-Jaya algorithm is tested on two standard power system test cases, representing static/dynamic cases respectively, with different complexity levels as shown in Table 1. Both the test cases have a non-convex, multimodal and stochastic objective function, where RESs uncertainty is modeled by using the random variables. In addition to these, Test Case II has a discontinuous objective function and the optimization variables are dynamically coupled in successive intervals through the ramp rate limits.

Test Case I: Four test example cases are created from the 10-thermal unit non-convex system with a load of 2000 MW [6]. The data is appended in Table A1 and Table A2. In Test Case I(A), the transmission losses are included in the model, which creates additional complexity in the equality constraint. Test Case I(B) is selected for result validation; it is similar to Test Case I(A) but the losses have been neglected here. In Test Case I(C), the second and third thermal generators in I(B) are replaced by wind power units. Test Case I(D) is constructed by adding one additional solar PV system to Test Case I(C); the data for the wind and solar units is listed in Table A.3 and Figure 4.

System I(A) is included in the study for benchmarking the proposed Ch-Jaya algorithm with previously reported results.

Test Case II: Test Case II(A) has all the complexities described earlier in this section and presented in Table 1. The limits, coefficients and ramp rates are given in Table A.4, and hourly demand variation is listed in Table A.5. Case II(B) is created to study the impact of RESs; hence thermal units eight and nine are replaced by wind power units and rest of the data is similar to Case IIA. Test Case II(C) has one additional solar system. The data for wind and solar units is the same as listed in Table A3 and Figure 4.

The physical representation of the problem is shown in Figure 5. The programs have been written in MATLAB R2013a and executed on an Intel Core i7 processor with a 3.40 GHz computer with 2 GB RAM.

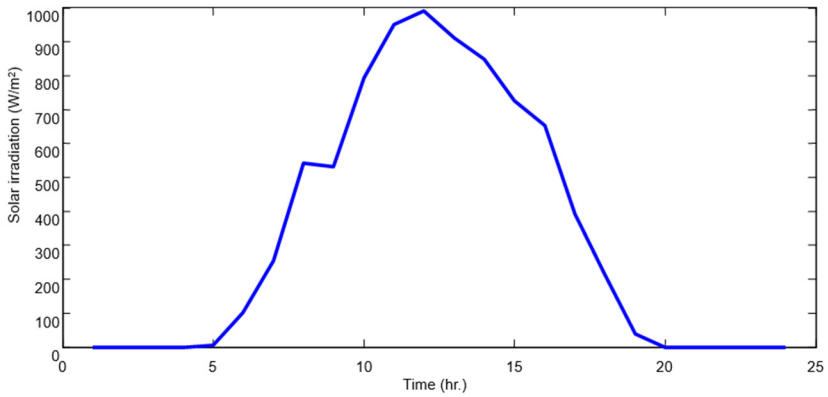

Figure 4. Solar radiation for a sample day.

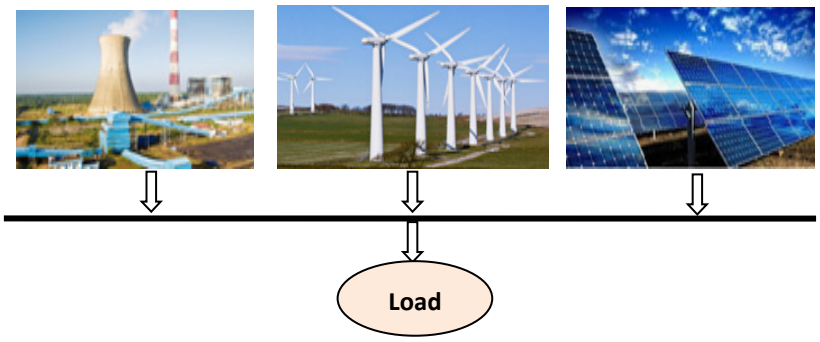

Figure 5. Schematic of Hybrid Thermal-wind-PV system.

Table 1. Test cases and their complexity.

Complexity level of test cases	I. 10-unit EED system [6]	II. 10-unit DEED system [42]
Non-convex multimodal	√	√
Ramp rate limit	X	√
Wind (Probabilistic model)	√	√
Solar (Probabilistic model)	√	√
Losses included (more complex equality constraints)	√	X

4.1. Setting of population size

In metaheuristic optimization methods, the population size must be set such that the best solution can be obtained within the least possible computational time. Studies were conducted on Test Case I by varying the population size from 10 to 100 with stopping criteria of 100 iterations. Based on the statistical analysis of results presented in Table 2, using 30 trials it is observed that a population size of 50 is optimal for this problem. Similarly, for Test Case II, the best population size is found to be 100.

Table 2. Selection of population size for test case IA.

NP	Min cost ($/h)	Ave cost ($/h)	Max cost ($/h)	S. D**	Comp. Time/iter. (Second)
10	111498.6776	111510.3160	111637.0302	13.1548	0.0009
20	111497.9356	111500.8442	111515.6150	2.8109	0.0016
50	111497.6480	111498.7725	111500.6211	0.2237	0.0039
100	111497.9698	111498.7453	111499.6834	0.1756	0.0075

** Standard deviation.

4.2. Selection of the best map

All chaotic maps described in Section 3.3 are embedded one by one with the Jaya algorithm and their effects were investigated on Test case IA. The statistical results of trials conducted with different chaotic maps are presented in Table 3. It is observed that the results for all the chaotic maps were almost similar, but with the lowest standard deviation, the tent map was found to be the most consistent as compared to the other maps. Therefore, for further analysis 'tent map' is used in the Ch-Jaya algorithm. However, the computational time gets increased as compared to the analysis carried out using the JAYA algorithm alone. The characteristics of the tent map along with other maps are presented in Figure 6. The convergence behavior of the Ch-Jaya algorithm is found to be superior to the Jaya algorithm as shown in Figure 7.

Table 3. Statistical comparison using different maps in Chaotic-Jaya (Test Case IA).

Sr. No.	Chaotic map	Best cost ($/hr)	Mean cost ($/hr)	Max cost ($/hr)	SD	Ave time/iter.(seconds)
1	Chebyshev	111497.6590	111498.1261	111500.6339	0.0978	0.0180
2	Circle	111497.6419	111497.7775	111498.2863	0.0301	0.0179
3	Gauss/mouse	111497.6354	111497.6646	111497.7993	0.0055	0.0182
4	Iterative	111497.6553	111497.7350	111497.9460	0.0131	0.0183
5	Logistic	111497.6419	111497.7897	111499.2180	0.0513	0.0183
6	Piecewise	111497.6416	111497.72205	111498.1050	0.0176	0.0181
7	Sine	111497.6343	111497.7277	111498.3407	0.02411	0.0183
8	Singer	111497.6518	111497.9670	111498.8708	0.0573	0.0185
9	Sinusoidal	111497.6596	111498.3263	111504.9584	0.24890	0.0183
10	Tent	111497.6312	111497.6403	111497.6545	0.0007	0.0177

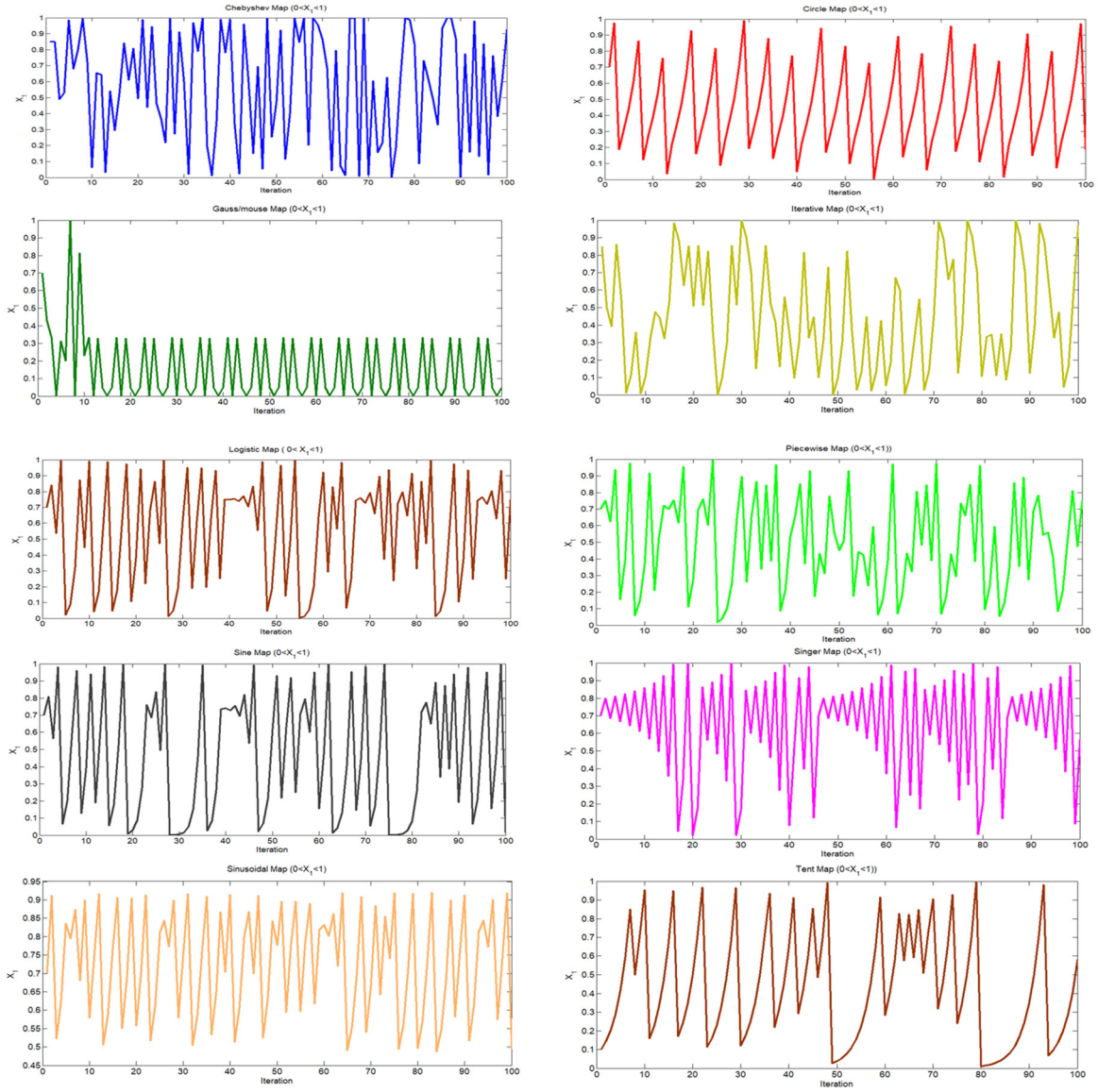

Figure 6. Variation of random parameters in Ch-Jaya through chaotic maps.

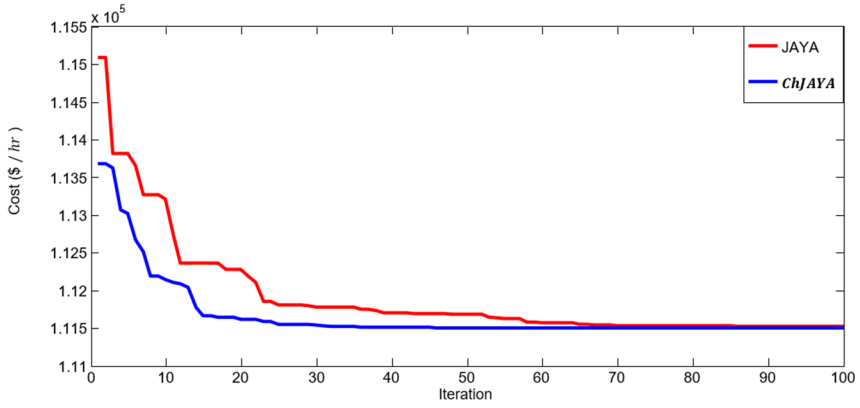

Figure 7. Cost convergence curve obtained by Jaya and C-Jaya for Test Case I.

4.3. Validation of results of Ch-Jaya for single/multi-objective static/dynamic test cases

The results of cost and emission optimization, for single objective cases, are compared and validated with previously published results of parallel hurricane optimization algorithm (PHOA) [43], DE [12] and chaotic improved harmony search CIHSA [6] in Table 4. The least cost solution obtained by the Ch-Jaya algorithm is $ 111497.6312/hr which is better than the other methods while all operational constraints are also satisfied. Table 4, also shows that the best emission 3932.2426 lb/hr is also obtained by using Ch-JAYA. These values are shown in bold.

The results of optimization of the bi-objective model given in Eq (30) are compared in Table 5 with GSA [5], MODE [12], NSGAII [12], enhanced multi-objective cultural algorithm (EMOCA) [44], flower pollination algorithm (FPA) [45] and CIHSA [6]. The results are comparable; the best cost $ 113246.5991/hr is found by Ch-JAYA while the lowest emission 3932.44734 lb/hr is reported by CIHSA [6].

Table 4. Validation of Ch-JAYA algorithm with published results (single objective (SO): Test Case IA).

Quantity	Best cost solution					Best emission solution			
	PHOA[43]	DE [12]	CIHSA [6]	JAYA	Ch-JAYA	DE [12]	CIHSA [6]	JAYA	Ch-JAYA
P1(MW)	34.2892	55	55.0000	54.9996	55.0000	55	55.000000	55	55
P2(MW)	79.5228	79.8063	80.0000	79.9997	80.0000	80	80.000000	79.9978	79.9998
P3(MW)	116.4348	106.8253	106.934727	107.0043	106.9381	80.5924	81.149904	81.1711	81.1362
P4(MW)	105.4548	102.8307	100.6003177	100.5125	100.5886	81.0233	81.359769	81.3775	81.3696
P5(MW)	110.0841	82.2418	81.476793	81.5588	81.4959	160	160.000000	159.9999	160.000
P6(MW)	108.3113	80.4352	83.026871	82.9670	83.0162	240	240.000000	239.9996	240.000
P7(MW)	285.1402	300	300.0000	299.9988	300.0000	292.7434	294.507931	294.5300	294.5035
P8(MW)	319.0626	340	340.0000	339.9998	340.0000	299.1214	297.268922	297.1563	297.2800
P9(MW)	457.6793	470	470.0000	469.9996	470.0000	394.5147	396.720288	396.8830	396.7832
P10(MW)	470.0000	469.8975	470.0000	469.9993	470.0000	398.6383	395.587840	395.4790	395.5220
PL(MW)	85.9792	NR	87.038709	87.0392	87.0388	NR	81.594656	81.5942	81.5943
TC ($/h)	112130	111500	111497.6310	111497.6480	111497.6312	116400	116412.5655	116412.5699	116412.60
TE(lb/h)	4520	4581.00	4572.27630	4572.1918	4572.2407	3923.40	3932.2433	3932.2443	3932.2426

NR: Not reported, PL: Power loss.

The optimal generation schedule for Test Case I(B), I(C) and I(D) is presented in Table 6 separately for cost and emission minimization. Furthermore, the statistical comparison for cost and emission obtained by Ch-JAYA and JAYA alone are compared in Table 6 (A) for Test Case I and in Table 7(A) for Test Case II. Here, it is observed that the performance of Ch-JAYA is better than JAYA in terms of either cost or emission minimization for all different cases considered for the analysis.

For case I(B), the cost $ 106170.3974/hr and emission 3650.7423 lb/hr, both computed by Ch-JAYA are superior to PHOA [43]. The minimum cost obtained by the Ch-JAYA algorithm for Test Case IIA using dynamic scheduling $ 2357135.0653, is shown to be better than the MBDE [27] algorithm $ 2482843.7918 in Table 7. Thus, the superior global search capability of Ch-Jaya is shown for the more complex Test Case II. Further analysis of Tables 6 and 7 for the impact of RESs is presented in the next section.

Table 5. Validation of best compromise solution of the Ch-JAYA algorithm (bi-objective: Test case I(A)).

Unit	EMOCA [44]	NSGAII [12]	MODE [12]	GSA [5]	FPA [45]	CIHSA [6]	JAYA	Ch-JAYA
P1(MW)	55	51.9515	54.9487	54.9992	53.188	55.000000	54.9879	55.0000
P2(MW)	80	67.2584	74.5821	79.9586	79.975	80.000000	79.8351	80.0000
P3(MW)	83.5594	73.6879	79.4294	79.4341	78.105	81.081501	86.4770	83.8795
P4(MW)	84.6031	91.3554	80.6875	85.0000	97.119	80.930292	85.2756	83.8340
P5(MW)	146.5632	134.0522	136.8551	142.1063	152.74	160.000000	139.9055	138.4066
P6(MW)	169.2481	174.9504	172.6393	166.5670	163.08	240.000000	157.4987	159.5070
P7(MW)	300	289.4350	283.8233	292.8749	258.61	290.800949	297.4614	298.0548
P8(MW)	317.3496	314.0556	316.3407	313.2387	302.22	296.689692	316.5739	314.9958
P9(MW)	412.9183	455.6978	448.5923	441.1775	433.21	398.842744	432.6969	433.0782
P10(MW)	434.3133	431.8054	436.4287	428.6306	466.07	398.331226	433.3181	437.4092
PL(MW)	83.56	84.25	84.33	83.9869	84.3	81.676404	84.0304	84.1653
TC ($/hr)	113445	113539	113484	113490	113370	116390.278321	113249.3676	113246.5991
TE (lb/hr)	4113.98	4130.2	4124.9	4111.4	3997.7	3932.4473	4133.2117	4133.3853

Table 6. Validation and comparison of optimal schedule with/without renewable integration.

Unit (MW)	Best cost solution				Best emission solution			
	PHOA[43] (Case IB)	Ch-JAYA Thermal (Case IB)	Thermal + wind (Case IC)	Thermal + wind + PV (Case ID)	PHOA[43] (Case IB)	Ch-JAYA Thermal (Case IB)	Thermal + wind (Case IC)	Thermal + wind + PV (Case ID)
P1	55	14.6927	10.0432	10.3934	55	11.5922	39.3307	45.5559
P2	80	79.9999	100.0000	100.0000	68.0479	78.0220	100.0000	100.0000
P3	98.2792	89.0902	100.0000	100.0000	73.4161	77.5040	100.0000	100.0000
P4	73.2943	80.2415	76.7470	62.9940	70.4446	77.5203	75.7202	70.7676
P5	70.2278	66.3405	63.6932	53.0084	160	160.0000	160.0000	159.9999
P6	72.7025	70.0003	70.0000	70.0000	240	240.0000	239.9941	240.0000
P7	270.4959	290.6202	279.1228	241.4460	275.2700	275.7460	265.8428	233.0241
P8	340	328.7074	315.4370	268.7833	289.1154	277.4743	267.5844	234.0780
P9	470	470.0000	470.0000	434.1333	371.9836	379.1481	367.8421	328.5067
P10	470	470.0000	470.0000	464.8209	396.7219	379.5854	368.0165	328.6240
PV1	--	---	---	75	--	--	---	75
PV2	--	---	---	75	--	--	---	75
PV_C($/hr)	--	---	---	6704.9000	--	--	---	6704.9000
W_C($/hr)	--	--	899.5334	899.5332	--	--	899.5334	899.5334
Th_C($/hr)	106210	106170.3974	102348.7811	93899.5937	111820	111866.7977	108222.7974	100334.0048
TC($/hr)		106170.3974	103248.3145	101504.0269	111820		109122.3309	107938.4382
TE(lb/hr)	4285.4729	4278.7877	3487.4606	2975.8779	3661.8815	3650.7423	2873.4340	2434.4654

Table 6(A). Statistical comparison of results for test Case-I.

Cost	Method	TC_{min}	TC_{mean}	TC_{max}	TC_{SD}
Thermal (I B)	Ch-JAYA	106170.3974	106170.3974	106170.3974	0.000
	JAYA	106170.5855	106170.8291	106171.3163	0.3597
Thermal +Wind (I C)	Ch-JAYA	103248.3145	103248.3145	103248.3145	0.000
	JAYA	103248.3185	103248.84764	103249.8093	0.55689
Thermal +Wind +PV (I D)	Ch-JAYA	101504.0269	101504.0269	101504.0269	0.000
	JAYA	101504.5935	101505.118375	101506.6807	0.9642
Emission	Method	E_{min}	E_{min}	E_{min}	E_{min}
Thermal (I B)	Ch-JAYA	3650.7423	3650.7423	3650.7423	0.000
	JAYA	3650.7455	3664.9977	3680.1238	13.8663
Thermal +Wind (I C)	Ch-JAYA	2873.4340	2873.4340	2873.4340	0.000
	JAYA	2873.4744	2878.1352	2890.4320	6.4882
Thermal +Wind +PV (I D)	Ch-JAYA	2434.4654	2434.4654	2434.4654	0.000
	JAYA	2437.4654	2463.2701	2512.8796	37.2171

Table 7. Optimal dynamic scheduling results with/without renewable energy integration (Test Case-II).

Description	Method	Cost minimization		Emission minimization		Cost and emission minimization	
		Cost ($)	Emission (lb)	Cost ($)	Emission (lb)	Cost ($)	Emission (lb)
Test Case IIA:	Ch-JAYA	2357135.0653	297005.3021	2539639.2507	270810.7558	2394132.0810	278171.8319
(Thermal system)	MBDE [27]	2482843.7918	-----	----	297235.4254	2475942.8.000	280507.6674
Test Case II B:	Ch-JAYA	2275684.9410	286249.2552	2447015.6637	256591.0774	2361299.2651	263475.4069
(Thermal+wind)							
Test Case II C: (Thermal+	Ch-JAYA	2200281.3668	258709.1654	2384872.7478	230769.1362	2240688.9885	240771.7490
wind +PV)							

Table 7(A). Statistical comparison of results for Test Case-II.

Cost	Method	TC_{min}	TC_{mean}	TC_{max}	TC_{SD}
Thermal (II A)	Ch-JAYA	2357135.0653	2357185.2055	2357228.1341	39.1856
	JAYA	2357143.2012	2357238.8978	2357305.9396	65.7636
	MBDE [27]	2482843.7918	2536958.9047	2595664.8001	---
Thermal + Wind (II B)	Ch-JAYA	2275684.941	2275794.2866	2275968.7051	90.1342
	JAYA	2275866.2582	2276399.9979	2276864.7177	180.1079
Thermal + Wind + PV	Ch-JAYA	2200281.3668	2200292.1569	2200329.9201	18.7739
(II C)	JAYA	2200286.855	2200387.7602	2201001.2758	104.6502
Emission	Method	E_{min}	E_{min}	E_{min}	E_{min}
Thermal (II A)	Ch-JAYA	270810.7558	270849.22645	270886.9112	45.3023
	JAYA	270819.3222	270862.3130	270955.822	55.0001
	MBDE [27]	297235.425431	3006001.8728	316941.7067	---
Thermal +Wind (II B)	Ch-JAYA	256591.0774	256678.8098	256782.2145	80.0806
	JAYA	256600.597268	256769.4573	256895.0774	136.5168
Thermal +Wind +PV	Ch-JAYA	230769.1362	230791.84022	230881.3668	47.1869
(II C)	JAYA	230771.9084	230842.99605	230975.3772	81.6702

4.4. Effect of RESs integration on cost and emission (single objective analysis)

From Table 6, it can be observed that as compared to the thermal system (Test Case IB), the reduction in cost with wind integration is found to be $ 2922.0829/hr (2.75% per hour) and with wind-solar integration is $ 4666.3705/hr (4.39% per hour). When two wind farms were replaced with thermal units in Test Case I(C), the greenhouse emission was reduced to 2873.4340 lb/hr (21.29%) and by integrating wind and solar PV systems (Test Case I(D)) the emission is reduced to 2434.4654 lb/hr (33.31%) as compared to emission released by the thermal system alone. So, it is concluded that optimization of "emission only" results in a greater reduction in emission as compared to reduction in cost for "cost only" optimization cases.

Similarly, the best cost solutions from Table 7 can be compared for Test Case II(A), II(B) and II(C) respectively. It is observed that the optimal cost of generation in a day for the three test cases is found to be $ 2357135.0653, $ 2275684.9410 and $ 2200281.3668 respectively. Comparing the results, it is observed that there is a reduction of $ 81450.1243 (3.45% per day) in total cost due to the integration of two wind power units in Case II(B). For the hybrid wind-solar PV-thermal system, IIC, the cost saving is $ 156853.6985 (6.65% per day).

From Table 7 it is also observed that greenhouse emission is reduced from 270810.7558 to 256591.0774 lb in Test Case II(B) and to 230769.1362 lb for Test Case II(C), which amounts to a reduction of approximately 5.25% (due to replacement of thermal units by wind units) and 14.78% per day (when one solar unit is added) respectively.

4.5. Effect of RES integration for static/dynamic test cases (bi-objective analysis)

The impact of RES integration is shown in Table 8 by comparing the results of Test Case I(B), I(C) and I(D) considering the bi-objective model. It is observed that a reduction of $ 2989.2133/hr (2.77% per hour) in cost and $ 5141.307/hr (4.76% per hour) in emission is achieved by wind integration. When both wind and solar PV systems are integrated with the thermal system the reduction in cost and emission content was found to be $ 5141.307/hr (4.77%) and 1229.4157 lb/hr (31.71%) respectively as compared to the original thermal system.

For Test Case II, it is observed that the total cost is reduced by $ 32832.8159 (1.37% per day) in Test Case II(B) and $ 153443.0925 (6.40% per day) in Test Case IIC due to wind and wind-solar PV integration respectively. The emission content is reduced by 14696.425 lb (5.28%) for Test Case II(B) and 37400.0829 lb (13.44%) for Test Case II(C).

Table 8. Effect of renewable integration on best compromise solution for test case I.

Unit (MW)	Thermal	Thermal + Wind	Thermal + Wind + PV
P1	20.9275	23.7312	26.3369
P2	79.9996	100.0000	99.9999
P3	81.1851	99.9981	100.0000
P4	79.0380	77.8904	73.0557
P5	127.0308	123.2389	109.4966
P6	141.9648	137.0887	118.7713
P7	285.8607	280.0773	257.0533
P8	302.5896	294.1344	267.1088
P9	421.2271	412.9401	382.6090
P10	426.1043	418.7427	386.9054
PV1	---	---	75.0000
PV2	---	---	75.0000
PV_C	---	---	6704.9000
W_C	---	899.4238	899.5328
Th_C	107836.9544	103947.2172	95091.2145
TC	107836.9544	104847.7411	102695.6474
TE	3876.1238	3098.4094	2646.7081

4.6. Impact analysis of RES integration with different optimization goals

The percentage reduction in total cost and emission due to RES integration for single and bi-objective goals for static/dynamic test cases—Test Cases I and II, respectively—has been summarized and shown as a stacked bar chart in Figure 8. The results in Figure 8 clearly show that after the integration of RES, the percentage reduction in emission for both test cases is higher as compared to the percentage reduction in total cost. This is because the uncertainty cost of RES, in terms of reserve and penalty costs, is included in the model. The reduction in emission in Test Case II is found to be lesser as compared to Test Case I for the same conditions/goals. This is due to the dynamic ramp-rate constraints in the DEED problem in Test Case II. These constraints limit the ramping down of the thermal generation leading to reduced scheduling of RES. Hence, emission reduction is lesser as compared to the static conditions in Test Case I. The bi-objective optimization succeeds in reducing both, cost and emission and presents a reasonably good percentage reduction in both objectives for all the tested cases.

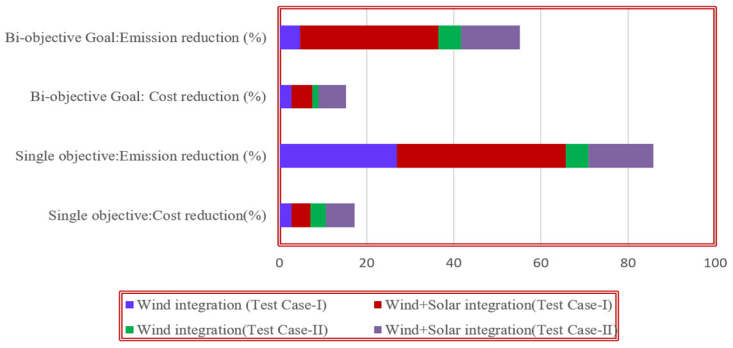

Figure 8. Percentage reduction in total cost and emission due to RES integration with different goals for static/dynamic test cases.

4.7. Optimal power sharing and constraint handling capability

The full optimal generation schedule obtained by Ch-JAYA under the three different optimization goals is available for test case I(A) in Tables 4 and 5, respectively. Tables 6 and 8 give the same for test cases I(B), I(C) and I(D). Similarly, Table 9 presents the optimal schedules for hybrid Test Case-II under the dynamic condition. From all these tables it can be seen that all operational constraints are fully satisfied by the proposed Ch-JAYA.

The optimal dynamic power sharing between solar, wind and thermal systems obtained by Ch-JAYA for best cost and best emission model for Test Case II(C) is shown in Figure 9(a,b). Similarly, the optimal power sharing under the bi-objective optimization of contradictory objectives is presented in Table 9. Here, all operational constraints are also fully satisfied.

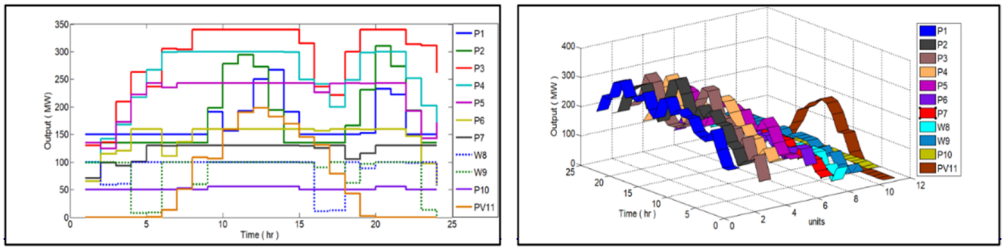

(a) Best cost solution (b) Best emission solution

Figure 9. Optimal dynamic generation schedule for the hybrid system, case II(C).

Table 9. Best compromise solution for the hybrid system: Test case II(C).

Hr	P1 (MW)	P2 (MW)	P3 (MW)	P4 (MW)	P5 (MW)	P6 (MW)	P7 (MW)	W8 (MW)	W9 (MW)	P10 (MW)	PV Share (MW)
1	150.0014	135.0001	191.8234	151.5584	118.5281	89.9424	129.6950	0.6593	18.4462	50.3457	0
2	150.2594	135.0005	116.1969	169.8757	115.1308	134.9533	129.4157	95.2536	8.4065	55.5076	0
3	150.0018	144.3037	170.9945	119.9176	164.2224	148.1099	117.5870	99.9997	92.7767	50.0867	0
4	150.0061	214.2780	250.8108	113.6353	204.4053	111.2748	129.7704	100.0000	81.8171	50.0022	0
5	156.4759	214.9372	241.5891	163.3822	204.6265	140.3210	129.9154	99.9999	78.3711	50.3428	0.03888
6	151.4708	248.3874	215.6170	213.3768	243.0000	159.9998	129.9999	99.9986	100.0000	52.5487	13.601
7	151.4197	268.7914	178.7951	263.2757	243.0000	159.9985	129.9808	99.9999	99.9999	55.9990	50.74
8	150.0001	190.6894	252.5426	299.9989	242.5281	159.5676	129.9999	94.6370	97.7932	50.0032	108.24
9	169.9263	242.0545	317.1218	299.9997	242.9191	159.9994	129.9955	99.9996	99.9985	55.9056	106.08
10	184.4012	307.1239	339.9998	282.3602	242.6156	159.9994	129.6074	63.7359	99.9999	53.3767	158.78
11	264.1419	269.8161	293.8628	299.9984	242.9990	159.9962	129.9541	99.7928	99.7843	55.6544	190
12	259.3396	266.3450	339.9984	299.9999	242.9998	159.9268	129.7458	99.9215	99.9999	53.7233	198
13	197.0151	264.3825	339.9999	299.9998	243.0000	159.8219	130.0000	99.9993	99.9910	55.7905	182
14	155.8151	291.6280	282.1309	258.1326	242.9966	160.0000	129.5412	82.5117	99.9997	51.6042	169.64
15	196.7869	213.6477	208.4307	261.2499	242.9997	142.6472	129.9959	81.3642	99.9988	53.5390	145.34
16	178.3078	228.8341	210.8882	226.5601	204.8421	92.6599	115.3215	15.8511	99.7621	50.1731	130.8
17	150.0027	158.7912	260.0941	225.1065	183.0817	140.2208	129.7157	68.6940	32.8061	52.9072	78.58
18	150.2003	149.0089	266.3200	270.1136	209.5865	159.9966	129.9989	99.9958	99.7562	50.0032	43.02
19	175.5597	228.8108	339.9994	253.3853	231.0325	159.9911	129.6348	99.9178	99.9992	55.6931	1.9763
20	254.3194	290.4072	339.9998	299.9939	243.0000	159.9928	129.9995	99.9998	99.9996	54.2880	0
21	252.9620	243.0624	339.9998	299.9997	242.9997	159.6172	129.8155	99.9991	99.9999	55.5447	0
22	201.9526	179.6179	269.9255	256.2532	242.3204	121.1640	100.9190	99.9989	100.0000	55.8485	0
23	150.0083	135.0017	189.9457	206.3243	192.3238	151.9635	70.9248	88.3861	97.1195	50.0023	0
24	150.0012	135.0005	210.9407	237.2007	156.4406	149.3306	56.4945	38.2114	0.2879	50.0919	0
Total cost: $ 2240688.9885, Emission: 240771.7490 (lb), Thermal cost: $ 2171546.8197, PV_cost: $ 68930, Wind cost: $ 212.1688											

4.8. Trade-off solutions computed by Ch-Jaya

In bi-objective optimization of contradictory objectives, there are many competing solutions and the decision maker selects the best suitable solution based on case-specific constraints set by economic or environmental limitations and guidelines. Figures 10 and 11 present the multiple trade-off solutions for Case I and Case II obtained by Ch-Jaya. It can be seen that Ch-Jaya has produced solutions that cover the full spread of cost-emission solution space, between the two extreme points marked by the best cost and best emission solutions.

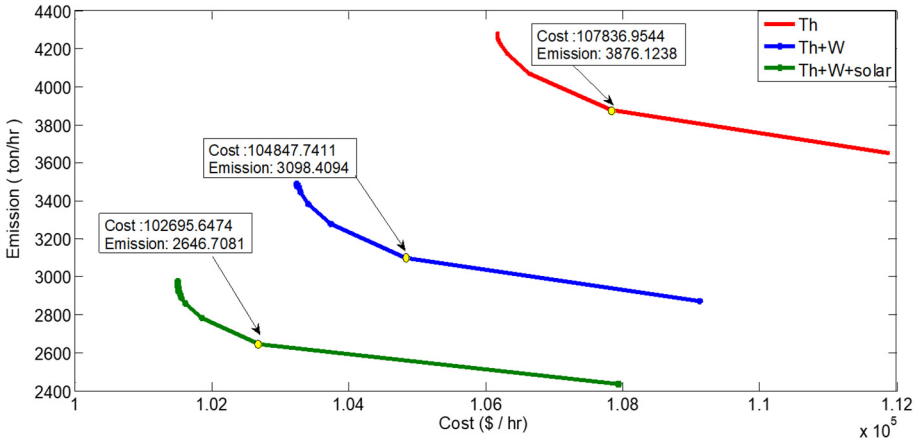

Figure 10. Comparison of Pareto-fronts for Test Case I(B), I(C) and I(D).

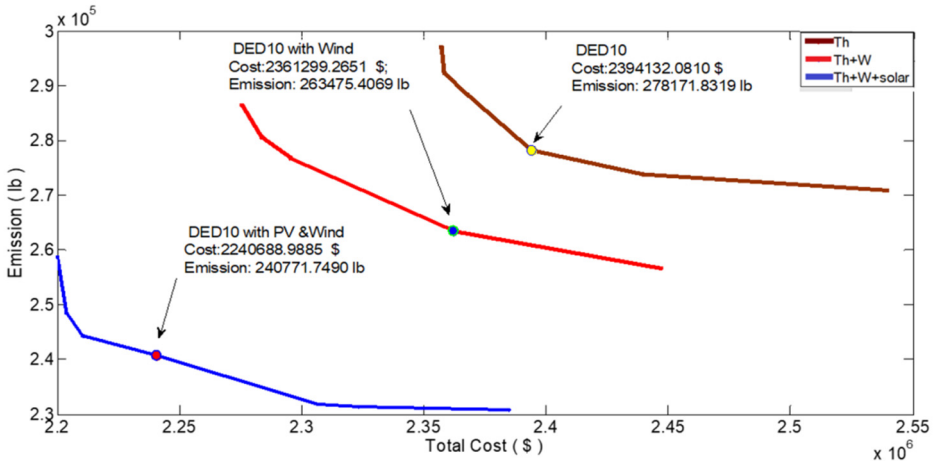

Figure 11. Comparison of Pareto-fronts for Test Case II(A), II(B) and II(C).

5. Conclusions

A modified JAYA algorithm is developed with different chaos maps for solving a non-convex, mixed integer, multimodal and stochastic problem with practical constraints. The effect of the integration of the uncertain nature of wind and solar PV systems on the optimal scheduling of two complex test systems is modeled using a probabilistic cost function, employing single/multi-objective

models. The performance of the proposed method is validated with published results for static/dynamic operating conditions, non-linear, discontinuous objective functions with multi-period, time-coupled constraints. The major findings are summarised as:

- The Jaya algorithm is an efficient population-based evolutionary algorithm that is free from convexity assumptions and any user-controlled program-specific tuning parameters.
- The results show that due to the integration of chaotic maps, the proposed Ch-JAYA has a superior convergence. The proposed Ch-JAYA algorithm is capable of producing feasible and credible results while handling complex and practical constraints.
- The bi-objective optimization succeeds in reducing both, cost and emission and presents a reasonably good percentage reduction in both objectives for all the tested cases.
- The effect of RES integration was investigated with single and bi-objective optimization goals and it was observed that the percentage reduction in emission for both the test cases is higher as compared to the percentage reduction in total cost.
- Results show that RES integration reduces the cost by about 2–4% but results in emission curtailment in the range of 20–33%.
- Considering simulation results under different test conditions it is observed that the Ch-JAYAalgorithm can provide credible and superior quality results and handle associated complex constraints as well as probabilistic functions in an efficient manner while satisfying all operational constraints.
- The fuzzy-min ranking approach is utilized to get the best solution for satisfying cost and emission.
- Pareto optimal solutions obtained under different test conditions provide various power scheduling options to GENCOs and the ISO can select scheduling options for minimizing either (i) total power generation cost, (ii) emissions or (iii) both simultaneously, to gain profit while protecting the environment.
- Power generation from wind turbine and solar PV systems is highly.
- This work may be extended with battery storage to improve power quality, suppress power fluctuation due to renewable energy resources and also to enhance supply security.

Acknowledgments

This research work was supported by “WOOSONG UNIVERSITY’s (Daejeon, Republic of Korea) Academic Research Funding-2023”.

Use of AI tools declaration

The authors declare they have not used Artificial Intelligence (AI) tools in the creation of this article.

Conflict of interest

Surender Reddy Salkuti is an editorial board member for AIMS Energy and was not involved in the editorial review or the decision to publish this article. All authors declare that there are no competing interests.

References

1. Aydin D, Özyön S, Yasar C, et al. (2014) Artificial bee colony algorithm with dynamic population size to combined economic and emission dispatch problem. *Int J Electr Power Energy Syst* 54: 144–153. https://doi.org/10.1016/j.ijepes.2013.06.020
2. Rajasomashekar S, Aravindhababu P (2012) Biogeography based optimization technique for best compromise solution of economic emission dispatch. *Swarm Evol Comp* 7: 47–57. https://doi.org/10.1016/j.swevo.2012.06.001
3. Qu BY, Zhua YS, Jiao YC, et al. (2018) A survey on multi-objective evolutionary algorithms for the solution of the environmental/economic dispatch problems. *Swarm Evol Comp* 38: 1–11. https://doi.org/10.1016/j.swevo.2017.06.002
4. Granelli GP, Montagna M, Pasini GL, et al. (1992) Emission constrained dynamic dispatch. *Electr Power Syst Res* 24: 56–64. https://doi.org/10.1016/0378-7796(92)90045-3
5. Guvenc U, Sonmez Y, Duman S, et al. (2012) Combined economic and emission dispatch solution using gravitational search algorithm. *Scientia Iranica D* 19: 1754–1762. https://doi.org/10.1016/j.scient.2012.02.030
6. Rezaiea H, Kazemi-Rahbar MH, Vahidi B, et al. (2019) Solution of combined economic and emission dispatch problem using a novel chaotic improved harmony search algorithm. *J Comp Design Eng* 6: 447–467. https://doi.org/10.1016/j.jcde.2018.08.001
7. Gonidakis D, Vlachos A (2019) A new sine cosine algorithm for economic and emission dispatch problems with price penalty factors. *J Inf Optim Sci* 40: 679−697. https://doi.org/10.1080/02522667.2018.1453667
8. Goudarzi A, Li Y, Xiang J (2020) A hybrid non-linear time-varying double-weighted particle swarm optimization for solving non-convex combined environmental economic dispatch problem. *Appl Soft Comp* 86: 105894. https://doi.org/10.1016/j.asoc.2019.105894
9. Dubey HM, Pandit M, Panigrahi BK (2018) An overview and comparative analysis of recent bio-inspired optimization techniques for wind integrated multi-objective power dispatch. *Swarm Evol Comp* 38: 12–34. https://doi.org/10.1016/j.swevo.2017.07.012
10. Wang L, Singh C (2007)Environmental/economic power dispatch using a fuzzified multi-objective particle swarm optimization algorithm. *Electr Power Syst Res* 77: 1654–1664. https://doi.org/10.1016/j.epsr.2006.11.012
11. Abido MA (2009) Multiobjective particle swarm optimization for environmental/economic dispatch problem. *Electr Power Syst Res* 79: 1105–1113. https://doi.org/10.1016/j.epsr.2009.02.005
12. Basu M (2011) Economic environmental dispatch using multi-objective differential evolution. *Appl Soft Comp* 11: 2845–2853. https://doi.org/10.1016/j.asoc.2010.11.014
13. Bhattacharya A, Chattopadhyay PK (2011) Hybrid differential evolution with biogeography-based optimization algorithm for solution of economic emission load dispatch problems. *Expert Syst Appl* 38: 14001–14010. https://doi.org/10.1016/j.eswa.2011.04.208
14. Jiang S, Ji Z, Shen Y (2014)A novel hybrid particle swarm optimization and gravitational search algorithm for solving economic emission load dispatch problems with various practical constraints. *Int J Electr Power Energy Syst* 55: 628–644. https://doi.org/10.1016/j.ijepes.2013.10.006

15. Gong D, Zhang Y, Qi C (2010) Environmental/economic power dispatch using a hybrid multi-objective optimization algorithm. *Int J Electr Power Energy Syst* 32: 607–614. https://doi.org/10.1016/j.ijepes.2009.11.017
16. Hagh MT, Kalajahi SMS, Ghorbani N (2020) Solution to economic emission dispatch problem including wind farms using exchange market algorithm method. *Appl Soft Comp* 88: 106044. https://doi.org/10.1016/j.asoc.2019.106044
17. Reddy SS, Bijwe PR, Abhyankar AR (2013) Multi-objective market clearing of electrical energy, spinning reserves and emission for wind-thermal power system. *Int J Electr Power Energy Syst* 53: 782−794. https://doi.org/10.1016/j.ijepes.2013.05.050
18. Shilaja C, Ravi K (2017) Optimization of emission/economic dispatch using Euclidean affine flower pollination algorithm (eFPA) and binary FPA (BFPA) in solar photo voltaic generation. *Renewable Energy* 107: 550−566. https://doi.org/10.1016/j.renene.2017.02.021
19. Joshi PM, VermaHK (2019) An improved TLBO based economic dispatch of power generation through distributed energy resources considering environmental constraints. *Sustainable Energy Grids Netw* 18: 100207. https://doi.org/10.1016/j.segan.2019.100207
20. Chen M, Zeng G, Lu K (2019) Constrained multi-objective population extremal optimization based economic-emission dispatch incorporating renewable energy resources. *Renewable Energy* 143: 277−294. https://doi.org/10.1016/j.renene.2019.05.024
21. Basu M (2006) Particle swarm optimization based goal-attainment method for dynamic economic emission dispatch. *Electric Power Comp Syst* 34: 1015−1025. https://doi.org/10.1080/15325000600596759
22. Mason K, Duggan J, Howley E (2017) Multi-objective dynamic economic emission dispatch using particle swarm optimisation variants. *Neurocomputing* 270: 188−197. https://doi.org/10.1016/j.neucom.2017.03.086
23. Basu M (2008) Dynamic economic emission dispatch using nondominated sorting genetic algorithm-II. *Int J Electr Power Energy Syst* 30: 140–149. https://doi.org/10.1016/j.ijepes.2007.06.009
24. Pandit N, Tripathi A, Tapaswi S, et al. (2012) An improved bacterial foraging algorithm for combined static/dynamic environmental economic dispatch. *Appl Soft Comp* 12: 3500−3513. https://doi.org/10.1016/j.asoc.2012.06.011
25. Niknam T, Golestaneh F, Sadeghi MS (2012) θ-multiobjective teaching-learning-based optimization for dynamic economic emission dispatch. *IEEE Syst J* 6: 341−352. https://doi.org/10.1109/JSYST.2012.2183276
26. Mason K, Duggan J, Howley E (2018) A multi-objective neural network trained with differential evolution for dynamic economic emission dispatch. *Int J Electr Power Energy Syst* 100: 201–221. https://doi.org/10.1016/j.ijepes.2018.02.021
27. Shen X, Zou D, Duan N, et al. (2019) An efficient fitness-based differential evolution algorithm and a constraint handling technique for dynamic economic emission dispatch. *Energy* 186: 115801. https://doi.org/10.1016/j.energy.2019.07.131
28. Li Z, Zou D, Kong Z (2019) A harmony search variant and a useful constraint handling method for the dynamic economic emission dispatch problems considering transmission loss. *Eng Appl Artificial Intel* 84: 18–40. https://doi.org/10.1016/j.engappai.2019.05.005

29. Dubey HM, Pandit M, Panigrahi BK (2015) Hybrid flower pollination algorithm with time-varying fuzzy selection mechanism for wind integrated multi-objective dynamic economic dispatch. *Renewable Energy* 83: 188−202. https://doi.org/10.1016/j.renene.2015.04.034
30. Qu BY, Liang JJ, Zhu YS, et al. (2019) Solving dynamic economic emission dispatch problem considering wind power by multi-objective differential evolution with ensemble of selection method. *Nat Comput* 18: 695−703. https://doi.org/10.1007/s11047-016-9598-6
31. Padhi S, Panigrahi BP, Dash D (2020) Solving dynamic economic emission dispatch problem with uncertainty of wind and load using whale optimization algorithm. *J Inst Eng India Ser B* 101: 65−78. https://doi.org/10.1007/s40031-020-00435-y
32. Dubey SM, Dubey HM, Pandit M, et al. (2021) Multiobjective scheduling of hybrid renewable energy system using equilibrium optimization. *Energies* 14: 6376. https://doi.org/10.3390/en14196376
33. Nourianfar H, Abdi H (2023) Economic emission dispatch considering electric vehicles and wind power using enhanced multi-objective exchange market algorithm. *J Cleaner Prod* 415: 137805. https://doi.org/10.1016/j.jclepro.2023.137805
34. Lai W, Zheng X, Song Q, et al. (2022) Multi-objective membrane search algorithm: A new solution for economic emission dispatch. *Appl Energy* 326: 119969. https://doi.org/10.1016/j.apenergy.2022.119969
35. Mahdavi M, Jurado F, Ramos RAV, et al. (2023) Hybrid biomass, solar and wind electricity generation in rural areas of Fez-Meknes region in Morocco considering water consumption of animals and anaerobic digester. *Appl Energy* 343: 121253. https://doi.org/10.1016/j.apenergy.2023.121253
36. Mahdavi M, Awaafo A, Jurado F, et al. (2023) Wind, solar and biogas power generation in water-stressed areas of Morocco considering water and biomass availability constraints and carbon emission limits. *Energy* 282: 128756. https://doi.org/10.1016/j.energy.2023.128756
37. Wolpert DH, Macready WG (1997) No free lunch theorems for optimization. *IEEE Trans Evol Comput* 1: 67−82. https://doi.org/10.1109/4235.585893
38. Mirjalili S, Gandomi AH (2017) Chaotic gravitational constants for the gravitational search algorithm. *Appl Soft Comp* 53: 407–419. https://doi.org/10.1016/j.asoc.2017.01.008
39. Gandomi AH, Yang XS, Talatahari S, et al. (2013) Firefly algorithm with chaos. *Commun Nonlinear Sci Numer Simulat* 18: 89–98. https://doi.org/10.1016/j.cnsns.2012.06.009
40. Reddy SS, Bijwe PR, Abhyankar AR (2015) Real-time economic dispatch considering renewable power generation variability and uncertainty over scheduling period. *IEEE Syst J* 9: 1440−1451. https://doi.org/10.1109/JSYST.2014.2325967
41. Rao RV (2019) Jaya: An advanced optimization algorithm and its engineering applications. *Springer* ISBN: 978-3-319-78921-7. https://doi.org/10.1007/978-3-319-78922-4
42. Roy PK, Bhui S (2016) A multi-objective hybrid evolutionary algorithm for dynamic economic emission load dispatch. *Int Trans Electr Energ Syst* 26: 49−78. https://doi.org/10.1002/etep.2066
43. Allah RMR, El-Sehiemy RA, Wang GG (2018) A novel parallel hurricane optimization algorithm for secure emission/economic load dispatch solution. *Appl Soft Comput* 63: 206–222. https://doi.org/10.1016/j.asoc.2017.12.002
44. Zhang R, Zhou J, Mo L, et al. (2013) Economic environmental dispatch using an enhanced multi-objective cultural algorithm. *Electr Power Syst Res* 99: 18–29. https://doi.org/10.1016/j.epsr.2013.01.010

45. Abdelaziz AY, Ali ES, Abd Elazim SM (2016) Implementation of flower pollination algorithm for solving economic load dispatch and combined economic emission dispatch problems in power systems. *Energy* 101: 506−518. https://doi.org/10.1016/j.energy.2016.02. 041

Appendix

Table A1. Unit data for Test Case I (ten unit system) [6].

Unit	P_{min} (MW)	P_{max} (MW)	a $(\$/(MW)^2h)$	b $(\$/MWh)$	c $(\$/h)$	e $(\$/h)$	f $((rad/MW)$	α $(lb/(MW)^2h)$	β (lb/MWh)	γ (lb/h)	η (lb/h)	δ $(1/MW)$
1	10	55	0.12951	40.5407	1000.403	33	0.0174	4.702	−398.64	36000.12	0.25475	0.01234
2	20	80	0.10908	39.5804	950.606	25	0.0178	4.652	−395.24	35000.56	0.25475	0.01234
3	47	120	0.12511	36.5104	900.705	32	0.0162	4.652	−390.23	33000.56	0.25163	0.01215
4	20	130	0.12111	39.5104	800.705	30	0.0168	4.652	−390.23	33000.56	0.25163	0.01215
5	50	160	0.15247	38.539	756.799	30	0.0148	0.420	32.77	1385.93	0.2497	0.012
6	70	240	0.10587	46.1592	451.325	20	0.0163	0.420	32.77	1385.93	0.2497	0.012
7	60	300	0.03546	38.3055	1243.531	20	0.0152	0.680	−54.55	4026.69	0.248	0.0129
8	70	340	0.02803	40.3965	1049.998	30	0.0128	0.680	−54.55	4026.69	0.2499	0.01203
9	135	470	0.02111	36.3278	1658.569	60	0.0136	0.460	−51.12	4289.55	0.2547	0.01234
10	150	470	0.01799	38.2704	1356.659	40	0.0141	0.460	−51.12	4289.55	0.2547	0.01234

Table A2. B-Loss coefficients (ten unit system).

$$B_{ij} = \begin{bmatrix} 0.0049 & 0.0014 & 0.0015 & 0.0015 & 0.0016 & 0.0017 & 0.0017 & 0.0018 & 0.0019 & 0.002 \\ 0.0014 & 0.0045 & 0.0016 & 0.0016 & 0.0017 & 0.0015 & 0.0015 & 0.0016 & 0.0018 & 0.0018 \\ 0.0015 & 0.0016 & 0.0039 & 0.001 & 0.0012 & 0.0012 & 0.0014 & 0.0014 & 0.0016 & 0.0016 \\ 0.0015 & 0.0016 & 0.001 & 0.004 & 0.0014 & 0.001 & 0.0011 & 0.0012 & 0.0014 & 0.0015 \\ 0.0016 & 0.0017 & 0.0012 & 0.0014 & 0.0035 & 0.0011 & 0.0013 & 0.0013 & 0.0015 & 0.0016 \\ 0.0017 & 0.0015 & 0.0012 & 0.001 & 0.0011 & 0.0036 & 0.0012 & 0.0012 & 0.0014 & 0.0015 \\ 0.0017 & 0.0015 & 0.0014 & 0.0011 & 0.0013 & 0.0012 & 0.0038 & 0.0016 & 0.0016 & 0.0018 \\ 0.0018 & 0.0016 & 0.0014 & 0.0012 & 0.0013 & 0.0012 & 0.0016 & 0.004 & 0.0015 & 0.0016 \\ 0.0019 & 0.0018 & 0.0016 & 0.0014 & 0.0015 & 0.0014 & 0.0016 & 0.0015 & 0.0042 & 0.0019 \\ 0.002 & 0.0018 & 0.0016 & 0.0015 & 0.0016 & 0.0015 & 0.0018 & 0.0016 & 0.0019 & 0.0044 \end{bmatrix}$$

$$B_{ij} = B_{ij} \times 10^{-2}$$

Table A3. Data for solar PV unit and wind farm.

Type of system	No. of units	Rated power (MW/Unit)	b_w, or b_{pv}, $(\$/MWh)$	kp	kr	k	c	Vci (m/s^2)	Vr (m/s^2)	Vco (m/s^2)
Solar PV	2	100	40	5	5	1.5	5	-	-	-
Wind	2	100	40			2	10	5	15	45

Table A4. Unit data for Test Case II (ten unit system) [42].

$Unit$	P_{min} (MW)	P_{max} (MW)	UR (MW)	DR (MW)	a $(\$/(MW)^2h)$	b $(\$/MWh)$	c $(\$/h)$	e $(\$/h)$	f $((rad/MW)$	α $(lb/(MW)^2h)$	β (lb/MWh)	γ (lb/h)	η (lb/h)	δ $(1/MW)$
1	150	470	80	80	0.1524	38.5397	786.7988	450	0.041	0.0312	−2.4444	103.3908	0.5035	0.0207
2	135	470	80	80	0.1058	46.1591	451.3251	600	0.036	0.0312	−2.4444	103.3908	0.5035	0.0207
3	73	340	80	80	0.0280	40.3965	1049.9977	320	0.028	0.0509	−4.0695	300.3910	0.4968	0.0202
4	60	300	50	50	0.0354	38.3055	1243.5311	260	0.052	0.0509	−4.0695	300.3910	0.4968	0.0202
5	73	243	50	50	0.0211	36.3278	1658.5696	280	0.063	0.0344	−3.8132	320.0006	0.4972	0.0200
6	57	160	50	50	0.0179	38.2704	1356.6592	310	0.048	0.0344	−3.8132	320.0006	0.4972	0.0200
7	20	130	30	30	0.0121	36.5104	1450.7045	300	0.086	0.0465	−3.9023	330.0056	0.5163	0.0214
8	47	120	30	30	0.0121	36.5104	1450.7045	340	0.082	0.0465	−3.9023	330.0056	0.5163	0.0214
9	20	80	30	30	0.1090	39.5804	1455.6056	270	0.098	0.0465	−3.9524	350.0056	0.5475	0.0234
10	50	56	30	30	0.1295	40.5407	1469.4026	380	0.094	0.0470	−3.9864	360.0012	0.5475	0.0234

Table A5. Load data for Test Case II (ten unit system) [42].

Hour	Load (MW)	Hour	Load (MW)	Hour	Load (MW)	Hour	Load (MW)
1	1036	7	1702	13	2072	19	1776
2	1110	8	1776	14	1924	20	1972
3	1258	9	1924	15	1776	21	1924
4	1406	10	2022	16	1554	22	1628
5	1480	11	2106	17	1480	23	1332
6	1628	12	2150	18	1628	24	1184